Molecular Biology of the Cell
Vol. 15, 3406–3417, July 2004

Peroxisomal Membrane Proteins Contain Common Pex19p-binding Sites that Are an Integral Part of Their Targeting Signals[D]

Hanspeter Rottensteiner,*† Achim Kramer,†‡ Stephan Lorenzen,§ Katharina Stein,* Christiane Landgraf,‡ Rudolf Volkmer-Engert,‡‖ and Ralf Erdmann*‖

*Institut für Physiologische Chemie, Ruhr-Universität Bochum, 44780 Bochum, Germany; and ‡Institut für Medizinische Immunologie and §Institut für Biochemie, Universitätsklinikum Charité, 10115 Berlin, Germany

Submitted March 8, 2004; Revised April 26, 2004; Accepted April 27, 2004
Monitoring Editor: Howard Riezman

Targeting of peroxisomal membrane proteins (PMPs) is a multistep process that requires not only recognition of PMPs in the cytosol but also their insertion into the peroxisomal membrane. As a consequence, targeting signals of PMPs (mPTS) are rather complex. A candidate protein for the PMP recognition event is Pex19p, which interacts with most PMPs. However, the respective Pex19p-binding sites are ill-defined and it is currently disputed whether these sites are contained within mPTS. By using synthetic peptide scans and yeast two-hybrid analyses, we determined and characterized Pex19p-binding sites in Pex11p and Pex13p, two PMPs from *Saccharomyces cerevisiae*. The sites turned out to be composed of a short helical motif with a minimal length of 11 amino acids. With the acquired data, it proved possible to predict and experimentally verify Pex19p-binding sites in several other PMPs by applying a pattern search and a prediction matrix. A peroxisomally targeted Pex13p fragment became mislocalized to the endoplasmic reticulum in the absence of its Pex19p-binding site. By adding the heterologous binding site of Pex11p, peroxisomal targeting of the Pex13p fragment was restored. We conclude that Pex19p-binding sites are well-defined entities that represent an essential part of the mPTS.

INTRODUCTION

Peroxisomes are ubiquitous organelles of eukaryotic cells, whose proteins are imported posttranslationally. Matrix proteins are directed to peroxisomes by either of two targeting signals, a C-terminal PTS1 or an N-terminal PTS2. The topogenesis of peroxisomal membrane proteins (PMPs) is accomplished by yet another mechanism, because most of the peroxin mutants, characterized by their defect in the biogenesis of peroxisomes, exhibit a block in matrix protein import, but do import PMPs normally (Lazarow and Fujiki, 1985; Gould and Valle, 2000; Subramani *et al.*, 2000; Purdue and Lazarow, 2001; Eckert and Erdmann, 2003). To date, only three peroxins with a potential role in PMP targeting have been identified, namely Pex3p (Hettema *et al.*, 2000; South *et al.*, 2000), Pex16p in mammals (South and Gould, 1999; Honsho *et al.*, 2002), and Pex19p (Götte *et al.*, 1998; Matsuzono *et al.*, 1999; Snyder *et al.*, 1999; Soukupova *et al.*, 1999). In cells lacking any of these proteins, PMPs are either degraded or mistargeted to other subcellular compartments such as mitochondria, the endoplasmic reticulum (ER) and membranes of unknown origin (Ghaedi *et al.*, 2000; Hettema *et al.*, 2000; Sacksteder *et al.*, 2000).

In accordance with a distinct pathway, PMPs use neither PTS1 nor PTS2. The targeting signals of PMPs (mPTS) that direct and insert PMPs into the peroxisomal membrane have been determined for a number of PMPs of several species. Despite some differences, a picture emerged from these studies of a targeting signal consisting of one or more transmembrane domains in conjunction with a short sequence, which contains either a cluster of basic residues or a mixture of basic and hydrophobic amino acids (Dyer *et al.*, 1996; Baerends *et al.*, 2000b; Pause *et al.*, 2000; Honsho and Fujiki, 2001; Wang *et al.*, 2001; Honsho *et al.*, 2002; Biermanns *et al.*, 2003; Murphy *et al.*, 2003). Although some similarities among these basic sequences have been noted, a clear consensus could not yet be deduced. Noteworthy, some PMPs have been shown to contain multiple nonoverlapping mPTS (Fransen *et al.*, 2001; Jones *et al.*, 2001; Brosius *et al.*, 2002).

Targeting-specific elements of an mPTS are expected to be recognized by a specific import receptor (signal recognition factor). Among the three peroxins with a potential role in PMP targeting identified to date, only Pex19p possesses some features of an mPTS recognition factor, as it is largely cytosolic (Götte *et al.*, 1998) and interacts with a number of PMPs in all species tested (Sacksteder *et al.*, 2000; Snyder *et al.*, 2000; Fransen *et al.*, 2001). Evidence is accumulating that

Article published online ahead of print. Mol. Biol. Cell 10.1091/mbc.E04–03–0188. Article and publication date are available at www.molbiolcell.org/cgi/doi/10.1091/mbc.E04–03–0188.

[D] Online version of this article contains supporting material. Online version is available at www.molbiolcell.org.

† These authors contributed equally to this work.

‖ Corresponding authors. E-mail addresses: rve@charite.de and Ralf.Erdmann@ruhr-uni-bochum.de.

Abbreviations used: ER, endoplasmic reticulum; GFP, green fluorescent protein; PMP, peroxisomal membrane protein; mPTS, peroxisomal membrane protein targeting signal.

Table 1. Plasmids used

Plasmid	Description	Primer pair	Source or reference
pHPR131	ADH2pr-PTS2-DsRed		Stein *et al.* (2002)
pKat61	PEX19 in pPC86/SalI-SacI	RE171/172	This study
pKat79	PEX19 in pGex4T-2/BamHI-SalI	RE103/104	This study
pPC86-PEX14	PEX14 in pPC86		Albertini *et al.* (1997)
pKat31	PEX13 (1–151) in pPC97/SmaI-SpeI	RE25/32	This study
pKat32	PEX13 (1–166) in pPC97/SmaI-SpeI	RE25/33	This study
pKat33	PEX13 (1–264) in pPC97/SmaI-SpeI	RE25/34	This study
pKat38	PEX13 (1–386) in pPC97/SmaI-SpeI	RE25/38	This study
pKat39	PEX13 (151–386) in pPC97/SmaI-SpeI	RE26/38	This study
pKat40	PEX13 (166–386) in pPC97/SmaI-SpeI	RE27/38	This study
pKat42	PEX13 (280–386) in pPC97/SmaI-SpeI	RE29/38	This study
pKat143	PEX13 (173–233) in pPC97/SalI-NotI	RE560/561	This study
pKat144	PEX13 (221–310) in pPC97/SalI-NotI	RE562/563	This study
pKat145	PEX13 (173–258) in pPC97/SalI-NotI	RE560/564	This study
pHPR281	PEX13 (1–386) L207A in pPC97	RE25/38	This study
pHPR229	PEX13 (1–386) L207P in pPC97	RE25/38	This study
pHPR221	PEX13 (173–258) L207A in pPC97	RE560/564	This study
pHPR262	PEX13 (173–258) L207P in pPC97	RE560/564	This study
pKat71	PEX11 (1–236) in pPC97/SalI-SacI	RE167/168	Rottensteiner *et al.* (2003)
pHPR274	PEX11 (1–236) L35G in pPC97	RE167/168	This study
pHPR275	PEX11 (1–236) L35P in pPC97	RE167/168	This study
pHPR231	PEX11 (1–50) in pPC97/SalI-SacI	RE700/701	This study
pHPR236	PEX11 (51–236) in pPC97/SalI-SacI	RE702/168	This study
pPC97/45	PEX25 (1–394) in pPC97/BglII-SalI	RE57/55	This study
pPC97/63	PEX25 (147–394) in pPC97/BglII-SalI	RE63/55	This study
pPC97/62	PEX25 (1–136) in pPC97/BglII-SacI	RE57/62	This study
pMS9	PEX13 (1–386) in pUG35/BamHI-EcoRI	RE432/435	Stein *et al.* (2002)
pMS15	PEX13 (166–264) in pUG35/BamHI-EcoRI	RE434/437	This study
pMS16	PEX13 (151–264) in pUG35/BamHI-EcoRI	RE433/437	This study
pMS22	PEX13 (166–310) in pUG35/BamHI-EcoRI	RE434/568	This study
pHPR227	PEX13 (166–310) L207A in pUG35	RE434/568	This study
pHPR228	PEX13 (166–310) L207P in pUG35	RE434/568	This study
pHPR241	PEX13 (200–310) in pUG35/BamHI-EcoRI	RE703/568	This study
pMS21	PEX13 (221–310) in pUG35/BamHI-EcoRI	RE567/568	This study
pHPR300	PEX13 (200–216) in pUG35/BamHI-HindIII	RE872/873	This study
pHPR293	PEX13 (200–264) in pUG35/BamHI-EcoRI	RE703/437	This study
pHPR252	PEX11 (28–40)-PEX13 (213–310) in pUG35	RE704/568	This study

Pex19p is indeed able to bind mPTS (Brosius *et al.*, 2002; Jones *et al.*, 2004), albeit other reports claimed that Pex19p binds some PMPs at regions that appear to be different from their sorting sequences (Snyder *et al.*, 2000; Fransen *et al.*, 2001, 2004). All these reports examined rather large PMP fragments for Pex19p binding and failed to detect any similarities between the different Pex19p-interacting fragments. It has even been suggested that Pex19p binds transmembrane domains of PMPs in a rather unspecific, chaperone-like manner (Jones *et al.*, 2004). To resolve these discrepancies, it is therefore crucial to understand the specific nature of the Pex19p-PMP interaction, which in turn should allow a more precise evaluation of its physiological role in the topogenesis of PMPs.

Here we identified the Pex19p-binding sites in a number of PMPs as short sequences that share a common motif. We established a matrix that allowed the sequence-based prediction of Pex19p-binding sites and verified the prediction in a proof of principle experiment. We further demonstrate that Pex19p-binding sites are integral and essential parts of mPTSs and we will discuss our findings in terms of Pex19p as a PMP import receptor.

MATERIALS AND METHODS

Strains and Media

Escherichia coli strain DH5α was used for all plasmid amplifications and isolations. *E. coli* strain C41 (DE3; J. Walker, Medical Research Council, Cambridge, UK) was used for heterologous expression of a recombinant GST-Pex19p fusion protein. For all yeast-two-hybrid assays, yeast strain PJ69-4A was used (P. James, Madison, WI). Localization of GFP-fusion proteins was analyzed in strain yHPR251, which expresses PTS2-DsRed from an integrated plasmid in strain UTL-7A (Stein *et al.*, 2002). Standard media for the cultivation of yeast and bacterial strains were prepared as described (Erdmann *et al.*, 1989; Sambrook *et al.*, 1989). Plates containing oleic acid (0.1% wt/vol) or ethanol (2%) as the sole carbon source were prepared according to Palmieri *et al.* (2001).

Plasmids and Oligonucleotides

Plasmids used are listed in Table 1, and the sequences of the oligonucleotides used are listed in Supplementary Table 1 (supplementary material). Genes or gene fragments were cloned into the various expression vectors using the restriction sites and primer pairs as indicated in Table 1. Point mutations were generated by overlap extension PCR. Specifically, the L207A and L207P mutations in Pex13p were introduced by using primers RE641/642 and RE643/644, respectively, in combination with the outer primer pair RE432/435. In case of the Pex11p mutations, primers RE742/743 (L35G) or RE744/745 (L35P) were combined with primer pair RE383/384. The resulting PCR products were cloned into *Eco*RV-cut pBluescript SK$^+$ (Stratagene, La Jolla, CA). These plasmids served as templates for further PCR reactions, designed

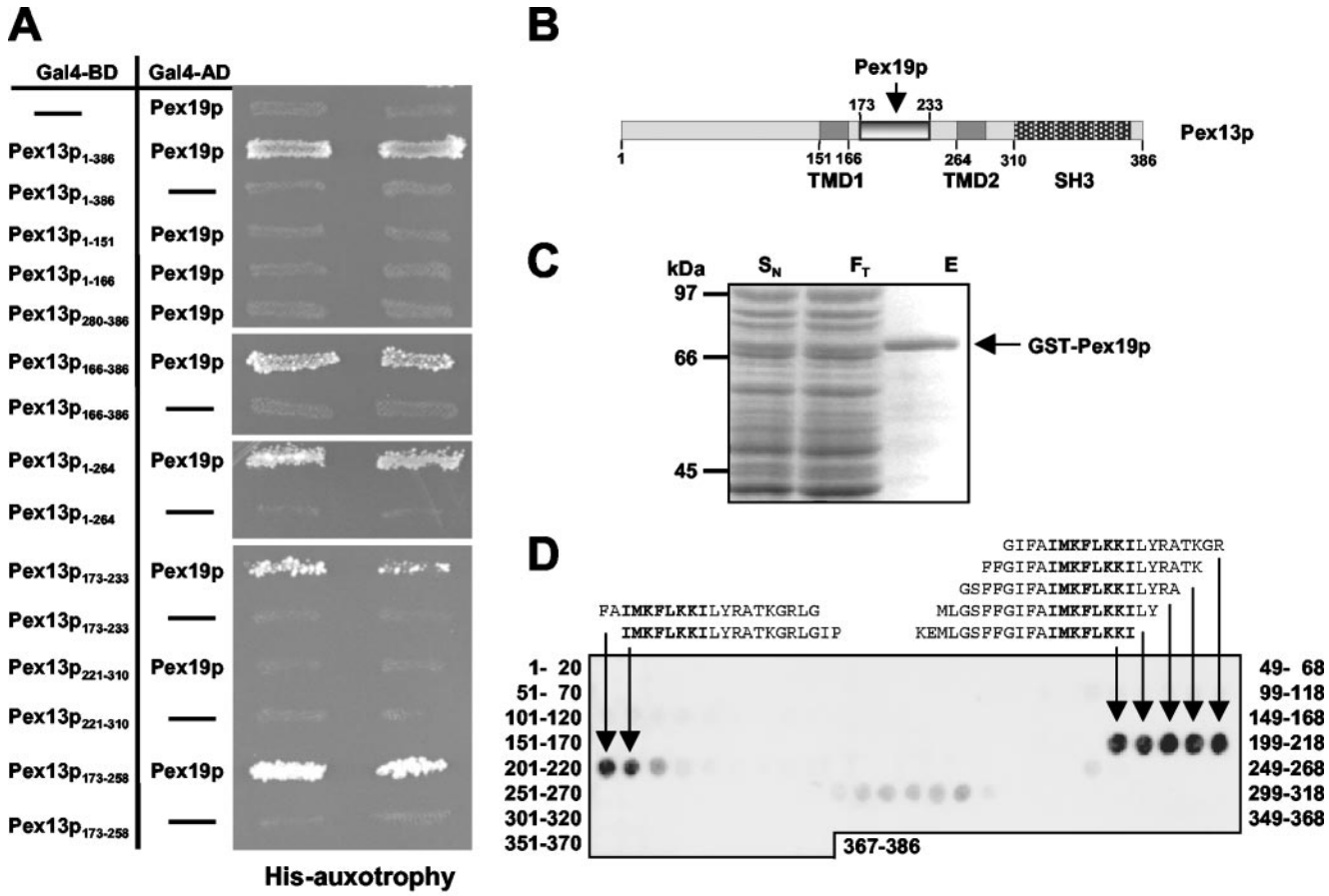

Figure 1. Identification of a Pex19p-binding site in Pex13p. (A) Interaction of Pex13p-fragments with Pex19p in a yeast two-hybrid assay. Full-length *PEX13* and various truncations thereof were fused to the *GAL4* binding domain (Gal4p-BD) in vector pPC97. The resulting plasmids were cotransformed into strain PJ69-4A with a pPC86-derived plasmid expressing a *PEX19-GAL4* activation domain (Gal4p-AD) fusion. As controls, empty pPC86 or pPC97 plasmids were used for transformation. Two independent transformants were tested for prototrophy on histidine adenine double dropout plates. Pex19p-Pex13p interactions were not tested in the opposite orientation because of autoactivity of the Pex19p-Gal4p-BD fusion protein. (B) Schematic view of Pex13p with its proposed transmembrane domains TMD1 and TMD2, the SH3 domain, and the Pex19p-binding site as narrowed down under A. Numbers indicate amino acid positions. (C) Purification of GST-Pex19p from *E. coli*. Shown is a Coomassie brilliant blue–stained gel with equal portions of the soluble extract expressing recombinant GST-Pex19p fusion protein (supernatant, S_N), the flow-through (F_T) after loading the extract onto a glutathione-Sepharose affinity column, and the eluate (E), which had been obtained by eluting bound protein with 10 mM glutathione. (D) In vitro binding of Pex19p to Pex13p-derived synthetic peptides. Overlapping 20-mer peptides with two-amino acid shifts between neighboring peptides representing the entire Pex13p were synthesized on cellulose membranes. Numbers denote the identity of the first and the last peptide of each line of the peptide array. The membrane was incubated with purified recombinant GST-Pex19p. Bound protein was visualized immunologically by using monoclonal anti-GST antibodies. Dark spots represent Pex13p peptides that had bound Pex19p. The corresponding peptide sequences are explicitly shown with the overlapping amino acids highlighted in bold.

to generate appropriate fragments with point mutations as indicated in Table 1. Correct nucleotide exchange was verified for all constructs by automated sequencing.

Yeast Two-Hybrid Assays

The two-hybrid assay was based on the method of Fields and Song (1989). Selected *PEX* genes or truncations thereof were fused to the DNA-binding domain or transcription-activation domain of Gal4p in the vectors pPC86 and pPC97 (Chevray and Nathans, 1992). To construct the Gal4p-AD-Pex13p fusions, *Eco*RI/*Spe*I fragments of the various *PEX13* fragments that had been amplified from genomic DNA were subcloned into the appropriately cut pPC86 (Table 1). To construct the Gal4p-BD-Pex13p fusions, the *PEX13* fragments were excised from the pPC86-PEX13 constructs with *Sma*I/*Spe*I and subcloned into *Sma*I/*Spe*I-digested pPC97 (Table 1). Cotransformation of two-hybrid plasmids into PJ69-4A was performed according to Schiestl and Gietz (1989). Double transformants were selected on SD synthetic medium without tryptophan and leucine. Transformed PJ69-4A was tested for concomitant histidine and adenine prototrophy by growth on selective plates lacking leucine, tryptophane, histidine, and adenine.

Subcellular Fractionation and Extraction of Peroxisomes

Differential centrifugation of postnuclear yeast lysates of oleic acid–induced cells at 25,000 × *g* was carried out essentially as described (Erdmann and Blobel, 1995). For successive protein extraction, organelles of the 25,000 × *g* pellet were lysed by incubation in high-salt buffer (10 mM Tris-HCl, pH 7.5; 0.5 M KCl) on ice for 1 h and were separated into pellet (HS P) and supernatant (HS S) fractions by centrifugation at 200,000 × *g* for 30 min at 4°C in an MLA130 rotor (Beckman Coulter, Fullerton, CA). The pellet fractions were further treated with alkaline carbonate buffer (0.1 M Na_2CO_3, pH 11.2) for 1 h on ice. The subsequent separation of membrane-bound (CO_3 P) and soluble (CO_3 S) fractions was achieved by a 30-min and 200,000 × *g* centrifugation step as described above. Equal portions of each fraction were separated by SDS-PAGE and analyzed by immunoblotting.

Antibodies and Western Blotting

The antibodies used were obtained from commercial sources or described previously, namely rabbit anti-Pex13p (Girzalsky *et al.*, 1999), anti-Pex11p (Erdmann and Blobel, 1995), anti-Pcs60p (Blobel and Erdmann, 1996), and anti–green fluorescent protein (GFP; W.H. Kunau, Bochum, Germany) as well

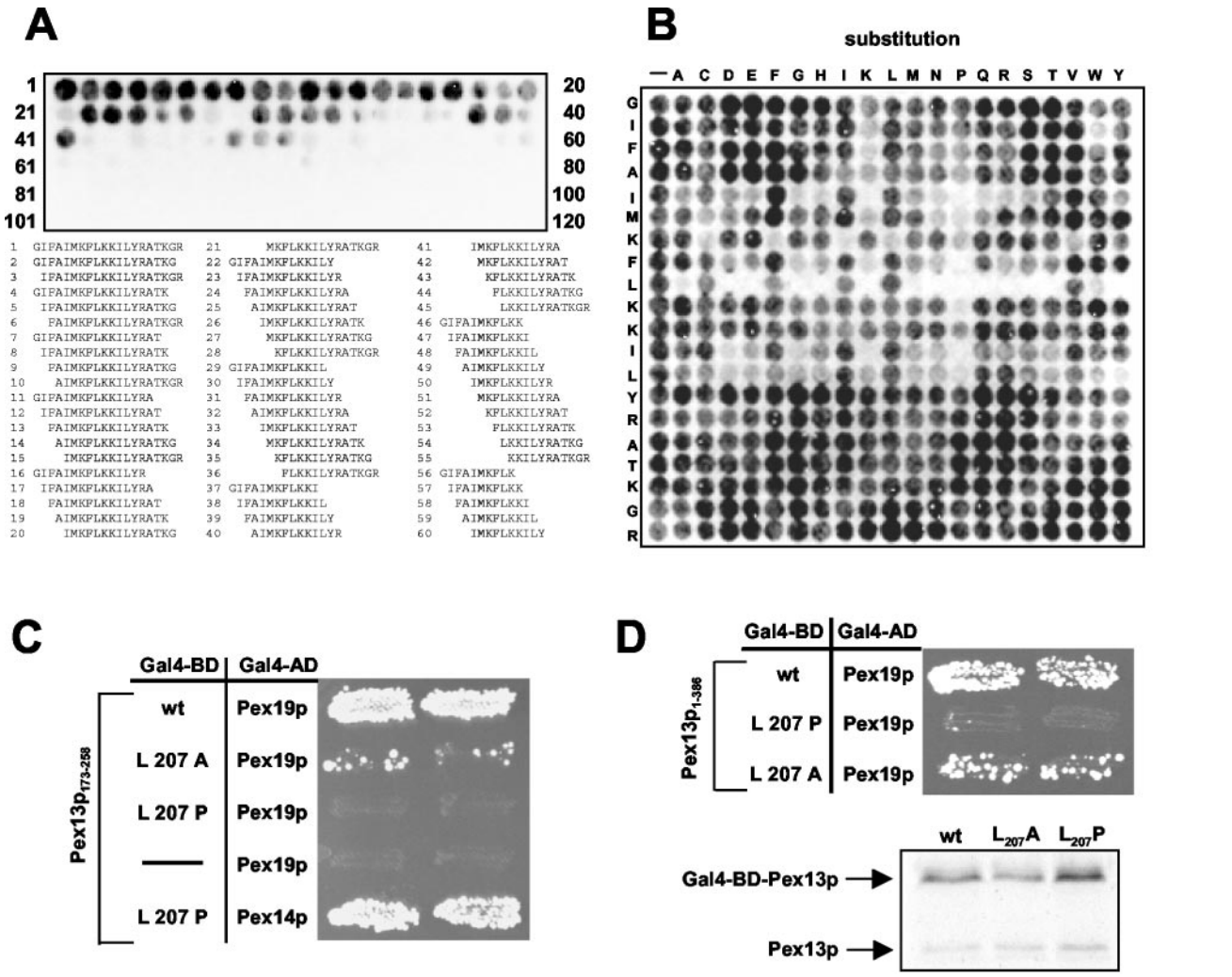

Figure 2. Characterization of the Pex19p-binding site in Pex13p. (A) Length analysis of the Pex19p-binding site. Peptides comprising systematic truncations of the original Pex19p-interacting peptide $Pex13p_{199–218}$ were synthesized on a cellulose membrane and tested for Pex19p interaction. Given below are the peptide sequences of the longest 60 peptides. (B) Substitution analysis. A synthesized peptide array with single amino acid substitutions within the $Pex13p_{199–218}$ peptide GIFAIMKFLKKILYRATKGR was tested for interaction with Pex19p. The various rows show peptides in which each amino acid of $Pex13p_{199–218}$ has been substituted by any of the indicated 20 amino acids, with the left-most peptide being the nonmutated wild-type peptide. Spots of reduced intensity represent peptides with reduced binding affinities for Pex19p. (C and D) The effect of mutating the Pex19p-binding site in vivo. A yeast two-hybrid assay was used to study the interaction of Pex19p with $Pex13p_{173–258}$ (C) or full-length Pex13p (D), both mutated at position L207. Expression of the mutated full-length Pex13p-Gal4p BD fusion proteins was tested by immunoblotting using anti-Pex13p antibodies (bottom panel). Native Pex13p served to demonstrate equal protein loading of the samples.

as monoclonal anti-GST (Sigma, Taufkirchen, Germany) and anti-yeast 3-phosphoglycerate kinase, Pgk1p (Molecular Probes, Eugene, OR) antibodies. Preparation of yeast whole-cell extracts and immunoblotting were performed according to standard procedures. Horseradish peroxidase–coupled anti-rabbit or anti-mouse IgGs, in combination with the ECL system (Amersham Pharmacia, Freiburg, Germany), were used to detect immunoreactive complexes.

Microscopy

Analysis of live cells for DsRed and GFP fluorescence was performed with a Zeiss Axioplan microscope and AxioVision 4.1 software (Zeiss, Jena, Germany). Before inspection, cells were grown for 2 days on solid minimal medium containing ethanol as a sole carbon source. Similar results were obtained when oleic acid was used as a sole carbon source (our unpublished observation).

Peptide Blot Assays

The peptide arrays were synthesized on modified cellulose membranes termed CAPE membranes (Landgraf *et al.*, 2004) using the SPOT synthesis technique (Reineke *et al.*, 2001). In vitro binding of Pex19p to the peptide libraries was analyzed as follows: the soluble fraction of glutathione *S*-transferase (GST)-Pex19p that had been expressed in C41 (DE3) from plasmid pKat79 (*PEX19* in pGEX4T-2) was bound for 2 h at 4°C on a glutathione-Sepharose 4B matrix (Amersham Pharmacia). After washing the matrix with 1× PBS (137 mM NaCl, 2.7 mM KCl, 4.3 mM $Na_2HPO_4×7\ H_2O$, 1.4 mM KH_2PO_4), the protein was eluted with 10 mM glutathione in 50 mM Tris HCl (pH 8). Eluted GST-Pex19p was analyzed by Coomassie brilliant blue staining. The purified protein was then added to the peptide-containing cellulose membrane in a concentration of 10 μg/ml. As control, 10 μg/ml GST (Sigma) was added to the membrane. Specifically bound protein was detected immunologically by using monoclonal anti-GST antibodies (Landgraf *et al.*, 2004). Spot intensities were quantified using the LumiImager (Roche, Basel, Switzerland).

Prediction of Pex19p-binding Sites

To train our prediction method, we used the quantified binding data from the substitution matrices of the most prominent binding peptides of Pex13p (GIFAIMKFLKKILYRATKGR) and Pex11p (KVLRLLQYLARFLAV). Addi-

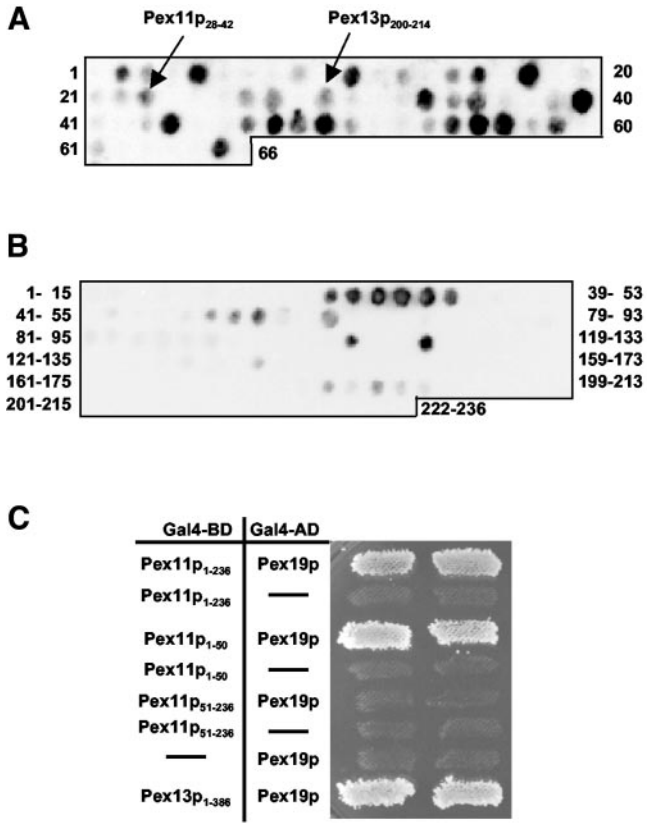

Figure 3. Identification of Pex19p-binding sites in other PMPs. (A) 15-mer peptides obtained from a pattern search for Pex13p-like Pex19p-binding sites within *S. cerevisiae* PMPs were synthesized and analyzed on a cellulose membrane for their ability to bind Pex19p in vitro. Spot numbers correspond to the peptide list given in Supplementary Table 2. The Pex19p-interacting peptides $Pex13p_{200-214}$ and $Pex11p_{28-42}$ are explicitly marked. (B) Peptide scan of Pex11p. Spots representing overlapping 15-mer Pex11p peptides with two-amino acid shifts between neighboring peptides were tested for interaction with Pex19p. The dominant series of interacting peptides covering amino acids 21–45 did include the $Pex11p_{28-42}$ peptide identified by the pattern search. (C) Confirmation of the Pex19p-binding site of Pex11p in vivo. Interaction of Pex19p with full-length $Pex11p_{1-236}$ (pKat71), the N-terminal 50 amino acids ($Pex11p_{1-50}$; pHPR231), and a C-terminal Pex11p fragment devoid of the major Pex19p-binding site ($Pex11p_{51-236}$; pHPR236) was analyzed by means of a yeast two-hybrid assay.

tionally, the binding data of the peptides from the pattern search hits (see Figure 3A) and data obtained with the identical peptides but with a [CILV] to A mutation (unpublished data) were included in the analysis. A prediction matrix regarding the nine core positions with the most relevant changes of binding affinity after amino acid substitution (IMKFLKKIL or LLQYLARFL, respectively) was generated, minimizing the sum of the squares of differences between measured and predicted values. For different peptide arrays, the predicted values were multiplied by a factor correcting for different sensitivity of detection that can be derived analytically. Minimizations were done using a commercial nonlinear optimizer (Frontline Systems, Solver DLL V 3.5, Incline Villa, NV; 1999). A stabilization of the matrix by introducing a penalty depending on the sum of the squares of matrix entries (Peters *et al.*, 2003) did not lead to a better description of binding profiles of several proteins generated by synthesis of displaced peptides, indicating that overfitting of the matrix to the data was not a problem.

RESULTS

Determination of the Pex19p-binding Site in Pex13p

Pex19p interacts with a number of peroxisomal membrane proteins. However, the features that determine functional

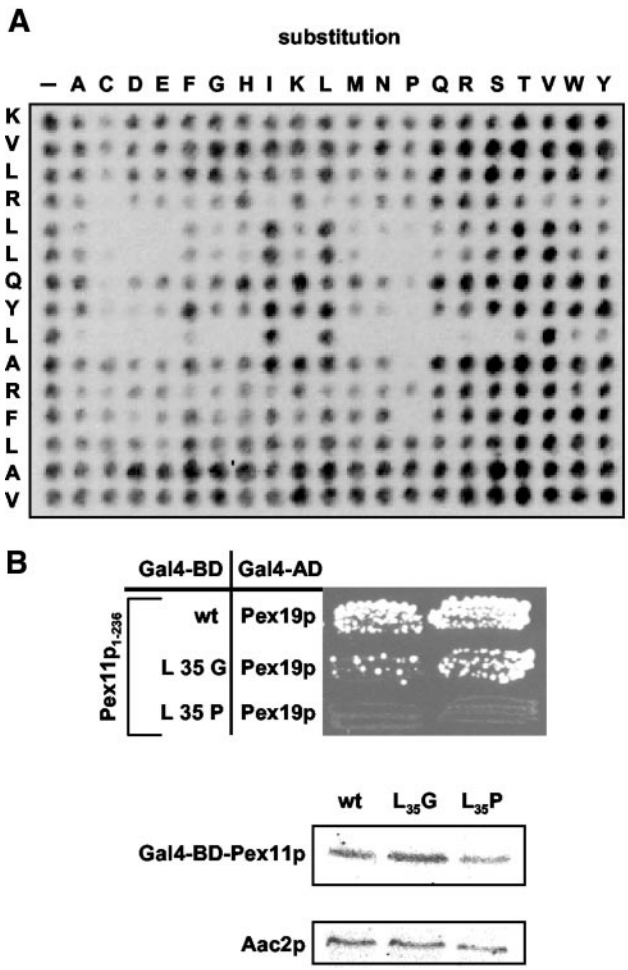

Figure 4. Characterization of the Pex19p-binding site in Pex11p. (A) Substitution analysis of the Pex19p-binding site in Pex11p. A synthetic peptide array based on the $Pex11p_{28-42}$ peptide sequence KVLRLLQYLARFLAV and containing all possible single amino acid substitutions was assayed for interaction with Pex19p. (B) The effect of mutating L35 of Pex11p in vivo. Two mutated versions of Pex11p, L35G (pHPR274) and L35P (pHPR275), were tested in a yeast two-hybrid assay for interaction with Pex19p. Given below is an expression control of the fusion proteins used in the assay.

Pex19p-binding sites are unknown. To unravel a potential regularity in such sites, we started with a dissection of *Saccharomyces cerevisiae* Pex13p, which we found to interact with Pex19p in a two-hybrid assay (Figure 1A). An internal region of ~100 amino acids of Pex13p, which is positioned between the two postulated transmembrane domains, was responsible for the Pex19p interaction, whereas the N- and C-termini of Pex13p yielded negative results in the assay. In a complementary approach, Pex19p was purified from *E. coli* as a recombinant GST fusion protein (Figure 1C). The purified protein was then incubated with a cellulose membrane containing an array of synthetic 20-mer peptides that were designed to represent the entire Pex13p sequence in an overlapping arrangement. Immunological detection of bound Pex19p-GST by monoclonal anti-GST antibodies resulted in a staining of serial spots that covered amino acids 191–222 of Pex13p containing a shared region (Figure 1D), whereas the control incubation of the cellulose membrane with purified GST did not result in significant binding to any of the peptides (unpublished data). Other weak spots ap-

Table 2. Predicted Pex19p-binding sites

PMP	Binding site[a]	Peak intensity[b]
Pex3p	25–50	7072
Pex3p	130–160	6898
Pex4p	125–145	1314
Pex8p	165–185	6806
Pex8p	280–300	12422
Pex10p	60–80	4186
Pex11p	20–40	4150
Pex11p	50–70	3059
Pex12p	180–225	4137
Pex12p	270–290	2866
Pex13p	195–215	6083
Pex15p	135–150	6656
Pex15p	335–350	5125
Pex17p	70–85	18202
Pex22p	120–135	3148
Pex25p	135–150	10449
Pex27p	120–140	18052
Pxa1p	30–50	9345
Pxa1p	200–225	6425
Pxa2p	115–160	13430

[a] Numbers designate the amino acid position of the predicted site.
[b] Arbitrary units.

peared at positions 89–128 and 271–298. However, neither a $Pex13p_{1–151}$ nor a $Pex13p_{221–310}$ fragment interacted with Pex19p in the two hybrid system. By using a $Pex13p_{173–233}$ fragment, the Pex19p binding site was further delimited also in vivo (Figure 1, A and B). These results indicated that Pex19p recognizes a distinct and linear sequence within Pex13p.

To determine the minimal length of a functional Pex19p binding site, the peak interacting Pex13p peptide 199–218 as well as all possible truncations thereof were synthesized and tested for Pex19p binding (Figure 2A). Three 11-mers with the core amino acids 203–211 were still able to bind Pex19p. Removing I_{203} or L_{211}, even in otherwise larger fragments, resulted in a loss of interaction. Nonetheless, because the 9-amino acid core was not sufficient for Pex19p binding, at least two additional flanking amino acids at either end are also required. The same 199–218 peptide formed the basis for a substitution matrix to reveal invariant or restricted amino acid positions within the sequence. Peptides each with a single amino acid substitution were exhaustively synthesized and again tested for Pex19p interaction (Figure 2B). Evidently, the core sequence of 9 amino acids, IMKFLKKIL emerged, flanking residues could be substituted without loss of binding. In addition to the important I_{203} and L_{211} residues also L_{207} turned out to be largely invariant, i.e., could only be replaced by other hydrophobic residues. Moreover, the basic residue K_{205} was not allowed to be substituted with the hydrophobic amino acids C, F, I, L, and V. Significantly, substitution of any of the nine core amino acids with proline impaired Pex19p binding, which suggests that the binding site is probably α-helical.

Introduction of a point mutation that leads to a substitution of leucine 207 to proline in the $Pex13p_{173–258}$ fragment resulted in a loss of Pex19p interaction also in vivo (Figure 2C). Correct folding of the mutated fragment was assured by demonstrating its interaction with Pex14p, which is accomplished by another region within this peptide (our unpublished observations). A less drastic mutation (L207A) did not abolish, but severely reduced the strength of the Pex19p interaction. Introducing the same point mutations into full-length Pex13p led to stably expressed Gal4p-binding domain fusion proteins (Figure 2D, bottom) whose abilities to interact with Pex19p resembled those of the mutant versions of the $Pex13p_{173–258}$ fragment (Figure 2D, top). Thus, Pex13p probably contains one predominant linear Pex19p-binding site.

A Common Theme within Pex19p-binding Sites

The Pex13p substitution matrix (Figure 2B) formed the basis for establishing a Pex19p-binding site pattern, which considered all amino acid substitutions within the nine amino acid core sequence that retained at least some Pex19p binding activity. Three flanking amino acids were included at either end of this core sequence so as to work with 15-mer peptides in this and following experiments. Searching the whole yeast proteome with this pattern, it became clear from the number of obtained hits that the stringency of the search was too low to truly identify Pex19p-binding sites. Nonetheless, restricting the analysis to peptides derived from PMPs, which are genuine Pex19p-binding targets, did yield putative Pex19p-binding sites. To that end, we synthesized those 15-mer peptides in question (Supplementary Table 2) and performed the in vitro Pex19p-binding assay (Figure 3A). Twenty-five of 66 peptides (38%) were considered positive for Pex19p interaction, whereas peptides originating from hits of an unrelated group of proteins showed an interaction in only 12 of 52 (23%) cases (unpublished data).

We chose Pex11p to exemplarily verify the obtained data, because a single positive peptide, comprising amino acids 28–42 with a signal intensity comparable to that of the Pex13p peptide, was obtained. In addition, a functional link does not exist between Pex11p and Pex13p. A peptide scan of the entire Pex11p clearly corroborated this peptide as being a Pex19p-binding sequence, because this sequence is contained within the obtained array of interacting spots comprising amino acids 21–45 (Figure 3B). To address the significance of the other sporadic or weakly stained spots appearing on the cellulose membrane, particularly those representing amino acids 51–69, Pex11p was dissected into an amino terminal 50 amino acid fragment and its corresponding C-terminal portion. Only full-length Pex11p and the $Pex11p_{1–50}$ fragment were able to interact with Pex19p in vivo (Figure 3C), indicating that amino acids 27–41 represent the major Pex19p-binding site in Pex11p.

A substitution analysis of this site revealed a core binding site of nine amino acids (R30 to F38), in which leucine residues at positions 31, 32, and 35 were most critical for binding (Figure 4A). Proline substitutions at any position within the core domain again interfered with Pex19p binding. We therefore substituted leucine 35 with proline in full-length Pex11p and analyzed the mutated protein's ability to interact with Pex19p in vivo (Figure 4B). Despite being stably expressed (bottom panel), $Pex11p_{L35P}$ lost its ability to interact with Pex19p. A substitution of the same leucine residue with glycine weakened, but did not abolish the Pex19p interaction. Thus, the data on Pex11p resembled those of Pex13p in that the Pex19p-binding sites of both proteins were composed of a distinct, small α-helical region, which contains hydrophobic and positively charged amino acids required for the efficient binding of Pex19p.

Prediction of Pex19p-binding Sites

To improve the accuracy of our Pex19p-binding site prediction, the peptide interaction data obtained from the Pex11p and Pex13p substitution analyses (Figures 4A and 2B) as well as the pattern search (Figure 3A) were quantified and

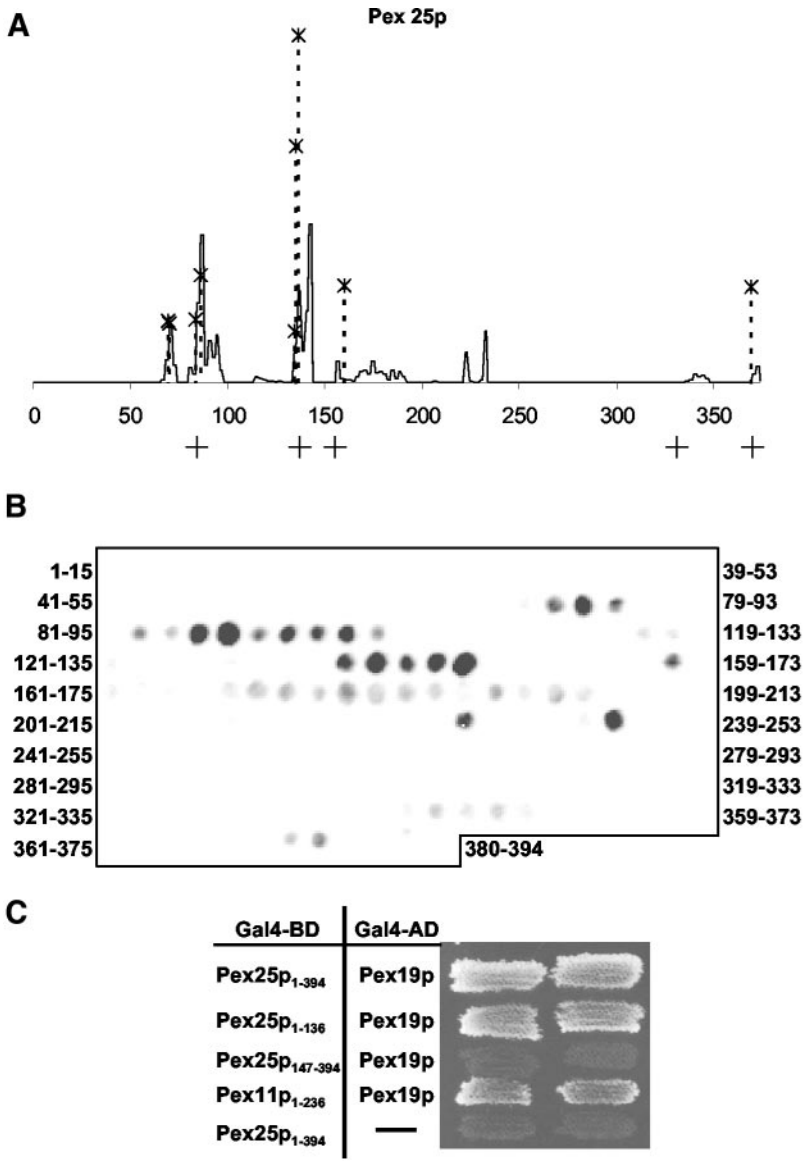

Figure 5. Prediction and identification of Pex19p-binding sites in Pex25p. (A) Binding site prediction. A prediction matrix for the central nine positions of a Pex19p-binding site was established (described in MATERIALS AND METHODS) and used to predict such sites in PMPs. Shown are the results for Pex25p. Hits are presented as dotted vertical lines, the magnitudes of which correlate with their calculated scores. Alternatively, the pattern search method was applied. Those hits are indicated by a (+). The continuous line corresponds with the intensities of the spots of the actual Pex25p peptide scan, which is shown in B. Note that the predictions obtained with the matrix are more precise than those with the pattern search. (C) In vivo analysis of the Pex25p-Pex19p interactions. Full-length Pex25p (pPC97/63) and the N-terminal $Pex25p_{1–136}$ fragment harboring two of the three Pex19p-binding sites (pPC97/62) as well as a C-terminal $Pex25p_{147–394}$ fragment lacking all three sites (pPC97/63) were tested for interaction with Pex19p in a yeast two-hybrid assay.

used to create a prediction matrix (see MATERIALS AND METHODS and Supplementary Table 3). In analogy to the peptide arrays used, the length of a Pex19p-binding site was fixed to 15 amino acids, but only the sequence of the 9 core positions was considered important. We subsequently screened PMPs against this matrix with the objective of predicting Pex19p-binding sites in these proteins. One to two eye-catching sites were found in most PMPs including the actual sites in Pex11p and Pex13p (Table 2). Interestingly, in most cases the proposed binding sites contained multiple high-scoring peptides. For a number of PMPs several hits of varying scores were obtained, suggestive of multiple Pex19p-binding sites. Pex25p, for instance, showed one major (amino acids 135–150) and two minor (amino acids 70–85 and 80–95) clusters of hits in the N-terminal half of the protein (Figure 5A).

To check the validity of this prediction, we determined the Pex19p-binding sites experimentally by using a Pex25p peptide scan. In line with multiple Pex19p-binding sites, several arrays of spots with significant intensities emerged (Figure 5B). Importantly, the observed spots correlated well with our matrix-based prediction, indicating that not only high-scoring hits may be true Pex19p-binding sites (Figure 5A). The Pex25p-Pex19p interactions were also verified by virtue of a two-hybrid assay (Figure 5C). Here, not only full-length Pex25p but also its N-terminal 136 amino acids were tested positive, showing that at least one of the two additional binding sites were functional in vivo. The C-terminal fragment $Pex25p_{147–394}$ lacking any of the determined Pex19p-binding sites failed to interact with Pex19p. This proof of principle clearly demonstrated the reliability of our Pex19p-binding site prediction for PMPs.

Targeting of PMPs Depends on Pex19p-binding Sites

To analyze whether Pex19p-binding sites play a role in the topogenesis of PMPs, the mPTS of Pex13p was determined by coexpression of various GFP-Pex13p fragments with PTS2-DsRed, a fluorescent peroxisomal marker protein. Expression of full-length Pex13p-GFP resulted in one or a few fluorescing spots that colocalized with PTS2-DsRed, indicating peroxisomal localization of the GFP fusion protein (Figure 6A). The design of subsequent Pex13p fragments took

into account the position of the Pex19p-binding site as well as the dispensability of the N-terminal 151 amino acids of Pex13p for targeting (Stein *et al.,* 2002). Even in the additional absence of the C-terminal SH3 domain and TMD2 ($Pex13p_{151–264}$), a largely peroxisomal localization was still observed (Figure 6A). However, by further removing TMD1 ($Pex13p_{166–264}$), colocalization with the peroxisomal marker protein was only rarely seen. Conversely, by adding TMD2 to this fragment ($Pex13p_{166–310}$) peroxisomal localization was regained, suggesting that at least one TMD is required for the efficient targeting of Pex13p (Figure 6A). Because the $Pex13p_{166–264}$ fragment contained the Pex19p-binding site, yet was inefficiently targeted to peroxisomes, it was concluded that Pex19p-binding sites are not sufficient for targeting. Indeed, fusions of GFP with the bare Pex19p-binding site, $Pex13p_{200–216}$ (Figure 6A) or with a slightly larger fragment ($Pex13p_{200–264}$, unpublished data) resulted in a nonperoxisomal staining. However, this was not surprising as there exists ample evidence in the literature that PMP-specific targeting sequences only work in conjunction with TMDs (Honsho and Fujiki, 2001; Wang *et al.,* 2001; Brosius *et al.,* 2002; Landgraf *et al.,* 2003). Thus, it was concluded that the identified mPTS of Pex13p is composed of a core region that contains the Pex19p-binding site plus a flanking TMD at any of its two ends.

The peroxisomally targeted $Pex13p_{166–310}$ fragment was mutated within the Pex19p-binding site at position L207. Introduction of the L207A mutation, which impaired Pex19p-binding (Figure 2, C and D), affected but did not completely abolish the peroxisomal targeting, with a significant fraction of the fragment being mislocalized to the cytosol and to membrane structures reminiscent of the ER (Figure 6B). The L207P mutation caused the fragment to be mainly localized to the ER, albeit peroxisomes were sometimes additionally labeled. Noticeable, both mutated fragments were similarly expressed like the wild-type fragment (unpublished data). Thus, diminished Pex19p binding did correlate with inefficient peroxisomal targeting.

To test targeting in the absence of the Pex19p site, we analyzed the localization of a $Pex13p_{200–310}$ fragment, which included the Pex19p-binding site and one ($Pex13p_{221–310}$) that was lacking it. As judged by the observed colocalization of $Pex13p_{200–310}$-GFP and PTS2-DsRed, the $Pex13p_{200–310}$ fragment retained the peroxisomal targeting information (Figure 6C). In sharp contrast, expression of $Pex13p_{221–310}$-GFP resulted in a staining of the ER, and colocalization with PTS2-DsRed was not observed (Figure 6C). These results showed that the region harboring the Pex19p-binding site was required for targeting of $Pex13p_{200–310}$. It remained possible, though, that the targeting information despite being located at position 200–220 constituted a distinct entity. The Pex19p-binding site of Pex13p was therefore exchanged by that of Pex11p. This chimera, which contained amino acids 28–40 of Pex11p and 213–310 of Pex13p, provoked a punctate GFP fluorescence in a significant number of cells. The peroxisomal identity of these spots could again be demonstrated by colabeling with PTS2-DsRed (Figure 6C), demonstrating the involvement of Pex19p-binding sites in the peroxisomal targeting of Pex13p.

To establish the subperoxisomal localization of the Pex13p fragments, subcellular fractionation and organelle extraction were carried out with these strains. The GFP fusions of both $Pex13p_{200–310}$ and $Pex11p_{28–40}$-$Pex13p_{213–310}$ were exclusively found in the 25,000 × *g* pellet enriched for peroxisomes (Figure 7A). The resulting pellets were subjected to high-salt extraction followed by a 200,000 × *g* centrifugation step to separate into a pellet enriched in membrane proteins and a supernatant containing matrix proteins and proteins modestly associated with membranes. Both Pex13p chimeras localized to the pellet fraction, indicating their tight association with the peroxisomal membrane (Figure 7B). The pellets obtained from high salt treatment were further extracted with carbonate at alkaline pH. Extraction with alkaline carbonate releases membrane-associated proteins, but not integral membrane proteins. Both Pex13p chimeras were recovered from the pellet fraction (Figure 7B). This result demonstrates that the GFP-Pex13p chimeras with a Pex19p-binding site and a TMD are indeed targeted to and inserted into the peroxisomal membrane.

DISCUSSION

Pex19p interacts with multiple PMPs (Götte *et al.,* 1998; Sacksteder *et al.,* 2000; Snyder *et al.,* 2000; Fransen *et al.,* 2001); however, precise Pex19p-binding sites have not yet been dissected and the physiological role of these interactions is under debate. We show here for the first time that Pex19p-binding sites represent short sequences that share a common motif and are integral parts of mPTSs and that these sites are required for the targeting of PMPs.

In a combined approach of in vivo two-hybrid analysis and in vitro peptide scanning studies, we could limit the Pex19p-binding site to an 11 amino acid region, which is characterized by conserved hydrophobic and positively charged amino acids. A subsequent test of the major Pex19p-binding site of Pex13p for its requirement for proper topogenesis revealed that in its absence, a Pex13p fragment was mistargeted to the ER. Moreover, replacement of this binding site by the corresponding binding site of Pex11p restored the peroxisomal targeting of the Pex13p fragment, therefore demonstrating 1) the contribution of the Pex19p-binding site to PMP targeting and 2) the functional interchangeability of Pex19p-binding sites between different PMPs. Neither the Pex19p-binding site of Pex13p nor the adjacent TMD alone was sufficient for peroxisomal membrane localization, which required the presence of both elements. It is well known that TMDs are crucial for the membrane localization of PMPs (Baerends *et al.,* 2000a; Honsho and Fujiki, 2001; Jones *et al.,* 2001; Wang *et al.,* 2001), without obligatorily providing specific targeting information. Accordingly, the mPTS of PMPs consists of at least two elements: 1) the Pex19p binding site, which might provide the targeting information and 2) an adjacent transmembrane span, which is required for the insertion and permanent anchoring of PMPs into the peroxisomal membrane.

The identified Pex19p-binding site is characterized by the presence of rather invariant basic amino acids that are surrounded by hydrophobic amino acids that seem to be placed in a certain distance to each other. Because proline residues are not allowed within this region, the binding site is likely to acquire an α-helical conformation. Our systematic analysis of the Pex19p-binding sites of yeast PMPs enabled us to generate a prediction matrix, which now allows prediction of the Pex19p-binding sites in other PMPs (Table 2). We could demonstrate the reliability of the matrix-based prediction by demonstrating a good match of the predicted and experimentally detected Pex19p-binding sites of Pex25p. This result also demonstrated the occurrence of multiple binding sites in at least some PMPs as reported previously for mammalian Pmp34p and Pmp22p (Jones *et al.,* 2001; Brosius *et al.,* 2002). The only Pex19p-binding site in higher eukaryotes that has been characterized in detail so far is that of *Homo sapiens* Pex13p (Fransen *et al.,* 2001). Aligning the Pex13p protein sequences from several species revealed that

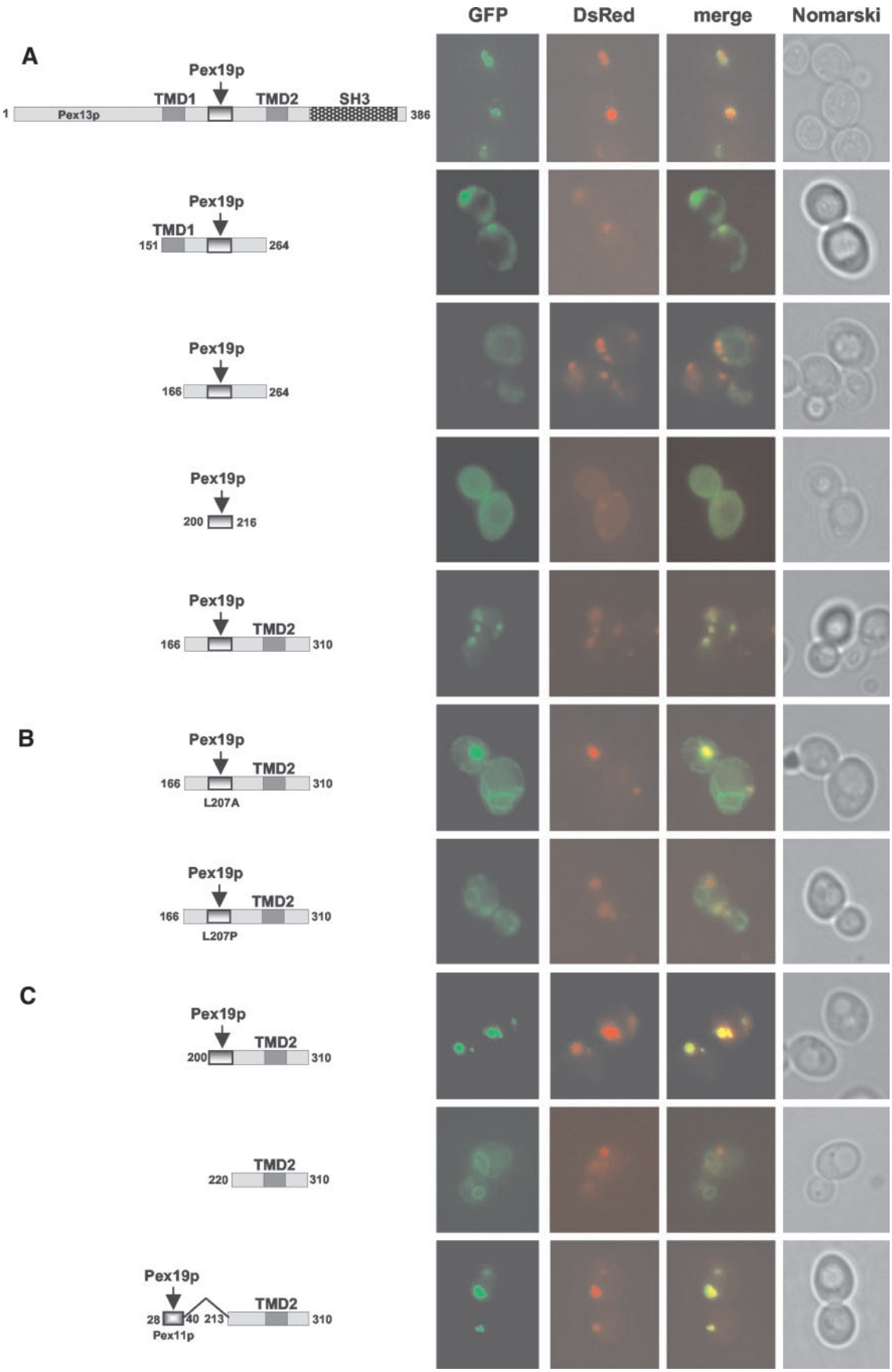
GFP
DsRed
merge
Nomarski
A
Pex19p
TMD1
TMD2
SH3
1
Pex13p
386
Pex19p
TMD1
151
264
Pex19p
166
264
Pex19p
200
216
Pex19p
TMD2
166
310
B
Pex19p
TMD2
166
310
L207A
Pex19p
TMD2
166
310
L207P
C
Pex19p
TMD2
200
310
TMD2
220
310
Pex19p
TMD2
28
40
213
310
Pex11p

Figure 6.

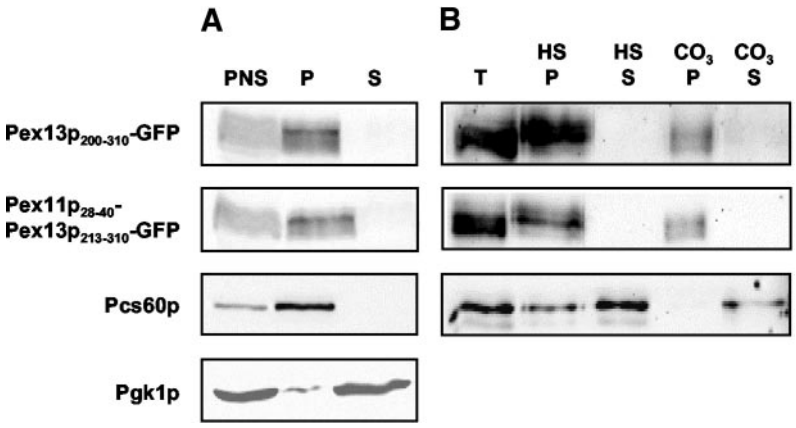

Figure 7. Insertion of the mPTS into the peroxisomal membrane. (A) Subcellular fractionation analysis. Transformants of the wild-type strain UTL-7A harboring plasmid pHPR241 ($Pex13p_{200-310}$-GFP) or pHPR252 (Pex11p28–40-$Pex13p_{213-310}$-GFP) were induced in oleic acid–containing medium. The resulting PNS fractions were separated into supernatant (S) and pellet (P) fractions by centrifugation at 25,000 × *g* for 30 min. Equivalent portions of each fraction were analyzed by immunoblotting. GFP-containing fusion proteins were detected by anti-GFP antibodies, whereas immunodecoration with anti-Pgk1p and anti-Pcs60p antibodies served to demonstrate the distribution of cytosol and peroxisomes, respectively. (B) Subperoxisomal fractionation analysis. The 25, 000 × *g* pellet fractions were resuspended in high-salt buffer (10 mM Tris-HCl, pH 7.5; 500 mM KCl), incubated for 1 h on ice, and separated into pellet (HS P) and soluble (HS S) fractions by a 30-min centrifugation step at 200,000 × *g*. Subsequently, the resulting pellet was resuspended in alkaline carbonate buffer (100 mM Na_2CO_3, pH 11.2), incubated for 1 h on ice, and subjected to centrifugation under identical conditions, yielding pellet fractions (CO_3 P) enriched for integral membrane proteins and soluble fractions (CO_3 S) enriched in tightly membrane-associated proteins. Pcs60p served as control for a high salt-extractable peroxisomal protein.

the Pex19p-binding site of *S. cerevisiae* represents a highly conserved region within the protein. More importantly, point mutations that abolished Pex19p binding of *Hs*Pex13p clustered exactly at the region corresponding to our identified Pex19p-binding site in *Sc*Pex13p. Remarkably, the random mutagenesis approach of *Hs*Pex13p carried out by Fransen *et al.* (2001) yielded the inactivating mutations L184S and I188T, which correspond to the critical positions I203 and L207 of *Sc*Pex13p, suggesting that the Pex19p-binding motif is evolutionarily conserved.

Recent data indicate that the presence of Pex19p increases the stability of newly synthesized PMPs, giving rise to a chaperone-like function of the protein (Jones *et al.*, 2004). As the binding site of Pex19p identified here contains a number of hydrophobic amino acids and our predicted Pex19p-binding sites did overlap or were even contained within TMDs of Pex3p, Pex12p, Pex15p, and Pxa2p, it is easily conceivable that binding of Pex19p does protect PMPs from misfolding. However, non-TMD Pex19p-binding sites were predicted for instance in the case of Pex10p, Pex13p, and Pex22p. Indeed, our data show that Pex19p does not simply bind to hydrophobic regions but rather binds to a well-defined sequence containing also charged amino acids, indicating that the Pex19p/PMP interaction does not resemble that of a typical chaperone. In support of a function of Pex19p as a PMP import receptor, the protein has been demonstrated to be required for PMP targeting and import (Hettema *et al.*, 2000; Jones *et al.*, 2004) and to interact with the mPTSs of several PMPs (Jones *et al.*, 2001; Brosius *et al.*, 2002). On the other hand, evidence has also been provided arguing against a function of Pex19p as an import receptor for newly synthesized PMPs (Snyder *et al.*, 2000; Fransen *et al.*, 2001, 2004). These opposing arguments are mainly based on the observations that Pex19p bound to PMP fragments, which did not seem to function as mPTS and vice versa. Some of these fragments obviously lacked a TMD. Because we could show that an mPTS requires a Pex19p-binding site plus TMDs, mistargeting of Pex19p-interacting fragments lacking a TMD is not unexpected. In the case of peroxisomal fragments that did not interact with Pex19p, several reasons might have caused the negative two-hybrid results, including a solubility problem of TMD-containing fragments. Nonetheless, additional Pex19p-independent targeting signals might have caused such observations and by no means do our results exclude the existence of such additional mPTS. In this respect, it is interesting to note that Pmp47p has been reported to contain two distinct mPTS, one being required for the targeting to mature and the other for the targeting to basal peroxisomes (Wang *et al.*, 2004). This might also explain why in *Yarrowia lipolytica* peroxisomes with small amounts of PMPs are discernible in a *pex19*Δ strain (Lambkin and Rachubinski, 2001).

Interestingly, the Pex19p-binding site motif resembles a motif of hydrophobic and basic amino acids that has been implicated recently in targeting of mammalian PMPs (Pause *et al.*, 2000; Brosius *et al.*, 2002; Biermanns *et al.*, 2003; Landgraf *et al.*, 2003). This opens the possibility that also in higher eukaryotes Pex19p binds the targeting-specific regions of mPTSs, which however needs to be studied in future work. That this could indeed be the case is supported by the interaction of *Hs*Pex19p with two nonoverlapping, peroxi-

Figure 6 (facing page). Dependence of peroxisomal targeting on Pex19p-binding sites. (A) Identification of an mPTS for Pex13p. Plasmids designed to express GFP fusions of the indicated Pex13p fragments were transformed into wild-type strain yHPR251, which expresses the peroxisomal marker protein PTS2-DsRed from an integrated expression vector (Stein *et al.*, 2002). The transformed strains were grown on ethanol plates for 2 days and examined for GFP- and DsRed-dependent fluorescence. Merged images reveal eventual peroxisomal colocalization of GFP fusion proteins with PTS2-DsRed. Nomarski images show the positions of the inspected cells. The fragments shown were expressed from the following plasmids: $Pex13p_{1-386}$ (pMS9); $Pex13p_{151-264}$ (pMS16); $Pex13p_{166-264}$ (pMS15); $Pex13p_{200-216}$ (pHPR300); and $Pex13p_{166-310}$ (pMS22). (B) Influence of Pex19p-binding site mutations on mPTS function. The mPTS of Pex13p ($Pex13p_{166-310}$) harboring a single point mutation in the Pex19p-binding site was fused to GFP and inspected for subcellular localization. Specifically, L207 was substituted with A (expressed from pHPR227) or P (pHPR228). (C) Requirement and interchangeability of a Pex19p-binding site within an mPTS. Analysis of the localization of GFP fusion proteins with Pex13p fragments, either including (pHPR241) or lacking (pMS21) the major Pex19p-binding site or having the Pex19p-binding site exchanged for that of Pex11p (pHPR252).

somally targeted fragments of Pmp22p from rat and humans, both of which contain the postulated mPTS (Brosius *et al.*, 2002).

In summary, our data demonstrate that a minimal Pex19p-binding site is composed of a conserved motif of 11 amino acids and that the developed prediction matrix proved useful in identifying such sites within other PMPs. Pex19p-binding sites were found to be an integral part of the mPTS, and we propose that in conjunction with one or more adjacent TMDs Pex19p-binding sites are sufficient for peroxisomal targeting and insertion of peroxisomal membrane proteins. Moreover, the fact that the Pex19p-binding site is part of an mPTS provides additional evidence for the functional role of Pex19p as the import receptor for peroxisomal membrane proteins.

ACKNOWLEDGMENTS

We thank M. Schärig for cloning and analyzing several Pex13p-GFP fusion constructs, E. Sonnenhol for cloning of the Pex25p two-hybrid constructs, and R. Rodemann for excellent technical assistance. This work was supported by grants of the Deutsche Forschungsgemeinschaft (SFB480 and SFB642) to R.E. and H.R. and Grant SFB449, TPZ1 to R.V.-E.

REFERENCES

Albertini, M., Rehling, P., Erdmann, R., Girzalsky, W., Kiel, J.A., Veenhuis, M., and Kunau, W.H. (1997). Pex14p, a peroxisomal membrane protein binding both receptors of the two PTS-dependent import pathways. Cell *89,* 83–92.

Baerends, R.J., Faber, K.N., Kiel, J.A., van der Klei, I.J., Harder, W., and Veenhuis, M. (2000a). Sorting and function of peroxisomal membrane proteins. FEMS Microbiol. Rev. *24,* 291–301.

Baerends, R.J., Faber, K.N., Kram, A.M., Kiel, J.A., van der Klei, I.J., and Veenhuis, M. (2000b). A stretch of positively charged amino acids at the N terminus of *Hansenula polymorpha* Pex3p is involved in incorporation of the protein into the peroxisomal membrane. J. Biol. Chem. *275,* 9986–9995.

Biermanns, M., von Laar, J., Brosius, U., and Gärtner, J. (2003). The peroxisomal membrane targeting elements of human peroxin 2 (PEX2). Eur J. Cell Biol. *82,* 155–162.

Blobel, F., and Erdmann, R. (1996). Identification of a yeast peroxisomal member of the family of AMP-binding proteins. Eur. J. Biochem. *240,* 468–476.

Brosius, U., Dehmel, T., and Gärtner, J. (2002). Two different targeting signals direct human peroxisomal membrane protein 22 to peroxisomes. J. Biol. Chem. *277,* 774–784.

Chevray, P.M., and Nathans, D. (1992). Protein interaction cloning in yeast: identification of mammalian proteins that react with the leucine zipper of Jun. Proc. Natl. Acad. Sci. USA *89,* 5789–5793.

Dyer, J.M., McNew, J.A., and Goodman, J.M. (1996). The sorting sequence of the peroxisomal integral membrane protein PMP47 is contained within a short hydrophilic loop. J. Cell Biol. *133,* 269–280.

Eckert, J.H., and Erdmann, R. (2003). Peroxisome biogenesis. Rev. Physiol. Biochem. Pharmacol. *147,* 75–121.

Erdmann, R., and Blobel, G. (1995). Giant peroxisomes in oleic acid-induced *Saccharomyces cerevisiae* lacking the peroxisomal membrane protein Pmp27p. J. Cell Biol. *128,* 509–523.

Erdmann, R., Veenhuis, M., Mertens, D., and Kunau, W.H. (1989). Isolation of peroxisome-deficient mutants of *Saccharomyces cerevisiae*. Proc. Natl. Acad. Sci. USA *86,* 5419–5423.

Fields, S., and Song, O. (1989). A novel genetic system to detect protein-protein interactions. Nature *340,* 245–246.

Fransen, M., Vastiau, I., Brees, C., Brys, V., Mannaerts, G.P., and Van Veldhoven, P.P. (2004). Potential role for Pex19p in assembly of PTS-receptor docking complexes. J. Biol. Chem. *279,* 12615–12624.

Fransen, M., Wylin, T., Brees, C., Mannaerts, G.P., and Van Veldhoven, P.P. (2001). Human Pex19p binds peroxisomal integral membrane proteins at regions distinct from their sorting sequences. Mol. Cell. Biol. *21,* 4413–4424.

Ghaedi, K., Tamura, S., Okumoto, K., Matsuzono, Y., and Fujiki, Y. (2000). The peroxin Pex3p initiates membrane assembly in peroxisome biogenesis. Mol. Biol. Cell *11,* 2085–2102.

Girzalsky, W., Rehling, P., Stein, K., Kipper, J., Blank, L., Kunau, W.H., and Erdmann, R. (1999). Involvement of Pex13p in Pex14p localization and peroxisomal targeting signal 2-dependent protein import into peroxisomes. J. Cell Biol. *144,* 1151–1162.

Götte, K., Girzalsky, W., Linkert, M., Baumgart, E., Kammerer, S., Kunau, W.H., and Erdmann, R. (1998). Pex19p, a farnesylated protein essential for peroxisome biogenesis. Mol. Cell. Biol. *18,* 616–628.

Gould, S.J., and Valle, D. (2000). Peroxisome biogenesis disorders: genetics and cell biology. Trends Genet. *16,* 340–345.

Hettema, E.H., Girzalsky, W., van Den Berg, M., Erdmann, R., and Distel, B. (2000). *Saccharomyces cerevisiae* Pex3p and Pex19p are required for proper localization and stability of peroxisomal membrane proteins. EMBO J. *19,* 223–233.

Honsho, M., and Fujiki, Y. (2001). Topogenesis of peroxisomal membrane protein requires a short, positively charged intervening-loop sequence and flanking hydrophobic segments. study using human membrane protein PMP34. J. Biol. Chem. *276,* 9375–9382.

Honsho, M., Hiroshige, T., and Fujiki, Y. (2002). The membrane biogenesis peroxin Pex16p. Topogenesis and functional roles in peroxisomal membrane assembly. J. Biol. Chem. *277,* 44513–44524.

Jones, J.M., Morrell, J.C., and Gould, S.J. (2001). Multiple distinct targeting signals in integral peroxisomal membrane proteins. J. Cell Biol. *153,* 1141–1150.

Jones, J.M., Morrell, J.C., and Gould, S.J. (2004). PEX19 is a predominantly cytosolic chaperone and import receptor for class 1 peroxisomal membrane proteins. J. Cell Biol. *164,* 57–67.

Lambkin, G.R., and Rachubinski, R.A. (2001). *Yarrowia lipolytica* cells mutant for the peroxisomal peroxin Pex19p contain structures resembling wild-type peroxisomes. Mol. Biol. Cell *12,* 3353–3364.

Landgraf, C., Panni, S., Montecchi-Palazzi, L., Castagnoli, L., Schneider-Mergener, J., Volkmer-Engert, R., and Cesareni, G. (2004). Protein interaction networks by proteome peptide scanning. PLoS Biol. *2,* E14.

Landgraf, P., Mayerhofer, P.U., Polanetz, R., Roscher, A.A., and Holzinger, A. (2003). Targeting of the human adrenoleukodystrophy protein to the peroxisomal membrane by an internal region containing a highly conserved motif. Eur. J. Cell Biol. *82,* 401–410.

Lazarow, P.B., and Fujiki, Y. (1985). Biogenesis of peroxisomes. Annu. Rev. Cell Biol. *1,* 489–530.

Matsuzono, Y. *et al.* (1999). Human PEX*19,* cDNA cloning by functional complementation, mutation analysis in a patient with Zellweger syndrome, and potential role in peroxisomal membrane assembly. Proc. Natl. Acad. Sci. USA *96,* 2116–2121.

Murphy, M.A., Phillipson, B.A., Baker, A., and Mullen, R.T. (2003). Characterization of the targeting signal of the Arabidopsis 22-kD integral peroxisomal membrane protein. Plant Physiol. *133,* 813–828.

Palmieri, L., Rottensteiner, H., Girzalsky, W., Scarcia, P., Palmieri, F., and Erdmann, R. (2001). Identification and functional reconstitution of the yeast peroxisomal adenine nucleotide transporter. EMBO J. *20,* 5049–5059.

Pause, B., Saffrich, R., Hunziker, A., Ansorge, W., and Just, W.W. (2000). Targeting of the 22 kDa integral peroxisomal membrane protein. FEBS Lett. *471,* 23–28.

Peters, B., Tong, W., Sidney, J., Sette, A., and Weng, Z. (2003). Examining the independent binding assumption for binding of peptide epitopes to MHC-I molecules. Bioinformatics *19,* 1765–1772.

Purdue, P.E., and Lazarow, P.B. (2001). Peroxisome biogenesis. Annu. Rev. Cell Dev. Biol. *17,* 701–752.

Reineke, U., Volkmer-Engert, R., and Schneider-Mergener, J. (2001). Applications of peptide arrays prepared by the SPOT-technology. Curr. Opin. Biotechnol. *12,* 59–64.

Rottensteiner, H., Stein, K., Sonnenhol, E., and Erdmann, R. (2003). Conserved function of Pex11p and the novel Pex25p and Pex27p in peroxisome biogenesis. Mol. Biol. Cell *14,* 4316–4328.

Sacksteder, K.A., Jones, J.M., South, S.T., Li, X., Liu, Y., and Gould, S.J. (2000). PEX19 binds multiple peroxisomal membrane proteins, is predominantly cytoplasmic, and is required for peroxisome membrane synthesis. J. Cell Biol. *148,* 931–944.

Sambrook, J., Fritsch, E.F., and Maniatis, T. (1989). Molecular Cloning: A Laboratory Manual. Cold Spring Harbor, NY: Cold Spring Harbor Laboratory Press.

Schiestl, R.H., and Gietz, R.D. (1989). High efficiency transformation of intact yeast cells using single stranded nucleic acids as a carrier. Curr. Genet. *16,* 339–346.

Snyder, W.B., Faber, K.N., Wenzel, T.J., Koller, A., Luers, G.H., Rangell, L., Keller, G.A., and Subramani, S. (1999). Pex19p interacts with Pex3p and Pex10p and is essential for peroxisome biogenesis in *Pichia pastoris.* Mol. Biol. Cell *10,* 1745–1761.

Snyder, W.B., Koller, A., Choy, A.J., and Subramani, S. (2000). The peroxin Pex19p interacts with multiple, integral membrane proteins at the peroxisomal membrane. J. Cell Biol. *149,* 1171–1178.

Soukupova, M., Sprenger, C., Gorgas, K., Kunau, W.H., and Dodt, G. (1999). Identification and characterization of the human peroxin PEX3. Eur J. Cell Biol. *78,* 357–374.

South, S.T., and Gould, S.J. (1999). Peroxisome synthesis in the absence of preexisting peroxisomes. J. Cell Biol. *144,* 255–266.

South, S.T., Sacksteder, K.A., Li, X., Liu, Y., and Gould, S.J. (2000). Inhibitors of COPI and COPII do not block PEX3-mediated peroxisome synthesis. J. Cell Biol. *149,* 1345–1360.

Stein, K., Schell-Steven, A., Erdmann, R., and Rottensteiner, H. (2002). Interactions of Pex7p and Pex18p/Pex21p with the peroxisomal docking machinery: implications for the first steps in PTS2 protein import. Mol. Cell. Biol. *22,* 6056–6069.

Subramani, S., Koller, A., and Snyder, W.B. (2000). Import of peroxisomal matrix and membrane proteins. Annu. Rev. Biochem. *69,* 399–418.

Wang, X., McMahon, M.A., Shelton, S.N., Nampaisansuk, M., Ballard, J.L., and Goodman, J.M. (2004). Multiple targeting modules on peroxisomal proteins are not redundant: discrete functions of targeting signals within Pmp47p and Pex8p. Mol. Biol. Cell *15,* 1702–1710.

Wang, X., Unruh, M.J., and Goodman, J.M. (2001). Discrete targeting signals direct Pmp47 to oleate-induced peroxisomes in *Saccharomyces cerevisiae*. J. Biol. Chem. *276,* 10897–10905.